Pergamon

CEMENT AND CONCRETE RESEARCH

Cement and Concrete Research 29 (1999) 27–36

Physicochemical study of the hydration process of an oil well cement slurry before setting

Paraskevi-Voula Vlachou, Jean-Michel Piau *

Laboratoire de Rhéologie, BP 53, Domaine Universitaire, 38041 Grenoble Cedex 9, France

Manuscript received 13 May 1997; accepted manuscript 5 October 1998

Abstract

This study deals with the basic phenomena that govern structural development during an oil well cement slurry hydration. This development has been followed from the mixing of cement with water to the beginning of setting. Scanning electron microscopy observations have been carried out, which revealed the form and structure of the hydration products as a function of the experimental conditions (e.g., temperature, stirring conditions). Results are correlated with X-ray diffraction analysis tests, to identify the chemical nature of crystalline formations observed.

Keywords: Oil well cement; Hydration; SEM; Temperature; Rheology

Cement slurries are reactive systems. They are continuously changing, physically and chemically. This study focuses on the microstructural and chemical evolution of an oil well cement slurry from the first minutes after mixing of cement powder with water until the beginning of setting.

A variety of physicochemical methods have been used to study the evolution of cement hydration. The most widely used are conduction calorimetry [1–3], quantitative X-ray diffraction analysis [4–7], thermal analysis techniques, such as differential scanning calorimetry, differential thermal analysis, and thermogravimetry [8], and electron microscopical techniques [4,9–16]. An extended review of the works concerning microscopy is given in reference [17]. Less popular techniques are solution analyses of the liquid phase [2], porosity measurements [4], surface area measurements [1], ultrasonic pulse velocity [18], impedance measurements [10], and electrical conductivity measurements [19,20]. Most of these methods are quite effective in describing the setting and after-setting hydration period, but they are more difficult to apply when studying the changes occurring from the time of mixing up to the beginning of setting. For example, heat and surface area development are widely used to determine the degree of hydration after the initial set, but both of these parameters show only very small changes before this point (i.e., during the period usually called "induction period"). Besides, most of these methods are concerned with either the solid or the liquid phase, but separation of the phases may cause alterations in their compositions. Consequently, particular attention must be paid to the experimental details before confidence can be gained in the results.

Scanning electron microscopy (SEM) was chosen in this study as a tool to obtain information about the development of microstructure during the early hydration period. Energy dispersive X-ray spectrometry was available in the electron microscope and was applied as an aid in identifying the chemical composition of some crystals and matrices observed. X-ray diffraction (XRD) analysis was performed in parallel, to identify the different products of the hydration reaction.

We used a Class G oil well cement, supplied by the German manufacturer Dyckerhoff. Cement particles are polymineralic, composed essentially of silicate and aluminate phases. Chemical composition and some physical characteristics of the cement used in this work are given in Table 1.

Several admixtures are used in the oil industry. They are agents that we add to the slurry in small quantities, to adjust their properties to the particular conditions of each well. In this work we used a modified lignosulfonate (ML) to delay setting and a hydroxyethylcellulose (HEC) to reduce filtration. These two additives were developed by Dowel Schlumberger and are available commercially under the names D801 and D59, respectively.

The composition of the slurries is given in Table 2. This

* Corresponding author. Tel.: (33) 4 76 82 51 70; Fax: (33) 4 76 82 51 64; E-mail: jmpiau@ujf-grenoble.fr.

0008-8846/99/$–see front matter
PII: S0008-8846(98)00182-3

Table 1
Chemical analysis and physical characteristics of Class G Dyckerhoff cement

Element	Ca	Si	Fe	Al	Mg	S	K	Na	LOI
% by weight	46.78	10.38	2.91	1.98	1.24	0.67	0.51	<1	0.92

Mean size = 17.8 μm
Density = 3230 kg/m^3

Table 2
Composition of the slurries

Water/cement ratio = 0.44
Mass conc. = 69%
Volume conc. = 41%
Density = 1920 kg/m^3
HEC = 0.55%*
M.L. = 0.28%*

* By weight dry cement.

composition was chosen because it provides slurries with an acceptable behavior for on-site use. The thickening time[1] of this formulation is given in Table 3.

Slurries were prepared as specified by the American Petroleum Institute [21]. A standardized Waring two-speed, propeller-type mixer was used. It was operated at 4000 rpm for about 15 seconds, during which cement and admixtures were added to the mix water, followed by 35 seconds at 12,000 rpm. After mixing, slurries are divided into two parts: the first part is hydrated under stirring at 150 rpm in a vertical paddle agitator; and the second part is hydrated at rest in a container.

This procedure is repeated at 20°C and 60°C. We followed the evolution of each of these parts, from right after mixing until the end of the thickening time.

Samples observed in this study are classified in Table 4, where experimental conditions are summarized. Whether the paste is agitated or not during hydration is designated by the presence or not of the letters "ag" in the classification name of each sample. The curing temperature (20°C or 60°C) is indicated at the end of each sample name. Samples of each formulation are numbered from 1 to 6. Number 1 corresponds to the beginning of the hydration and 6 corresponds to the end of the thickening time. Samples taken between these two points are numbered from 2 to 5 according to their age. For comparison we also report the fraction of the thickening time corresponding to each sample time.

1. Scanning electron microscopy results

1.1. Apparatus and methods

The microscope used for this study was the JEOL 6300F field emission electron microscope available at the Institut Français du Pétrole (IFP). It provides high resolution (1.5 nm at 30 kV on Au/C), and high performance and low noise at low accelerating voltages (7 nm at 1 kV), which makes it useful for fragile materials. The microscope is fitted with an energy dispersive X-ray analyzer (Link eXL), which enables the detection of all elements, including light elements such as C and O, despite of a low sensitivity for these two elements. The resolution of the local elemental analysis is about 1 μm in all directions, but it depends on the accelerating voltage and on the chemical nature of the analyzed area. It has to be noted that, due to the limited resolution of the local elemental analysis, when analyzing small particles, we also have a signal from the underlying or surrounding surfaces. These analyses, therefore, provide only qualitative indications of the composition of the examined area.

According to the consistency of the pastes, either a micropipe of about 3-mm extremity diameter or a small spatula was used to withdraw samples from the bulk cement paste. A small amount of cement paste (about 0.5 g) was put on an appropriate sample holder. It was then soaked in nitrogen slush. The frozen sample was fractured and subjected to a lyophilization program for 16 hours. Samples were slightly coated with platinum (a film of about 5 nm) and introduced into the SEM chamber for observation, under a high vacuum of about 10^{-5} torr. The analyses were conducted at 5 to 15 kV, depending on the charging effects.

To verify the reliability of our results and the absence of artifacts induced by the experimental protocol, we also used a second preparation method. This method consisted of adding acetone to the cement paste to remove water, then evaporating solvent to recover cement grains and hydration products. Samples prepared in this way are compared to the corresponding samples prepared by lyophilization in Fig. 1 and Figs. 11 and 12. These images confirm that the preparation method does not alter sample characteristics.

2. Discussion of the results

2.1. Anhydrous cement

Figure 2 shows micrographs of anhydrous cement powder. Cement grains of different shapes and sizes are unevenly mixed. Some energy dispersive X-ray microanalysis results are presented in this figure. Grain 1 gives a spectrum

[1] The thickening time of a slurry is a standardized parameter, defined as the time during which the slurry is sufficiently fluid to be pumped. A specific apparatus (the consistometer) is used for its determination. The operational procedure to be followed is contained in API specification 10, Section 8, Appendix E [21].

Table 3
Thickening times of the slurries

Temperature (°C)	20	60
Thickening time	20 h	5 h 30 min

Table 4
Classification of samples prepared for SEM viewing

Hydration conditions	Time of hydration (t)	t/(thickening time)	Sample classification name
Dry cement			Dry-cem
Stirred (60°C)	7 min	0.002	ag60-1
	1 h	0.18	ag60-3
	3 h	0.55	ag60-5
	5 h 30 min	1	ag60-6
Stagnant (60°C)	2 h	0.36	60-4
	5 h 30 min	1	60-6
Stirred (20°C)	5 min	0.004	ag20-1
	8 h 45 min	0.44	ag20-4
	20 h	1	ag20-6
Stagnant (20°C)	8 h 45 min	0.44	20-4
	20 h	1	20-6

of a silicate grain [22]. Grain 3 contains an aluminate phase and the grain 4 is a gypsum particle.

2.2. ag60

Just after mixing with water (Fig. 3) coarse particles are well dispersed. Some fine particles are aggregated. Polymeric admixtures are seen at this stage. They form filaments lying between the grains. A small quantity of hydration products is present in this sample. Small rod-like features are unevenly dispersed. They often appear in little clumps (points 6 and 7), which can be interpreted as indicating areas of enhanced reactivity. X-ray microanalysis reveals them to be rich in aluminum and sulfur. This could correspond to ettringite. However, the size of these aluminate regions is generally too small to be detected as a separate phase in X-ray microprobe analysis.

The following figures show the development of paste structure with time of hydration. Magnitude and quantity of rod-like crystals increase continuously with hydration time. They seem to precipitate in the interparticle spaces, on the basis of the through-solution mechanism. On the other hand, clumps of very tiny rod-like products keep appearing locally on the particle surfaces. They present the same qualitative composition as the bigger rods with a spreading of Al/S intensities ratios. The dispersion of the hydrates on the grain surfaces and away from them seems to account for the coexistence of the topochemical and the through-solution reaction mechanisms. Additives fade out with time.

Fig. 4 shows the sample taken at the beginning of the setting (at 5 h 30 min from mixing with water). Porosity is largely reduced in comparison with previous samples, and new crystal types appear. Crystals in the form of long slender needles or very thin plates piled up on each other appear in some areas. They are reminiscent of thin calcium hydroxide (portlandite) crystals, but their elementary analysis reveals some Si. In very high magnifications we can distinguish that the entire surface of the particles is covered by fibrillar material, which is probably the C-S-H gel (point 7).

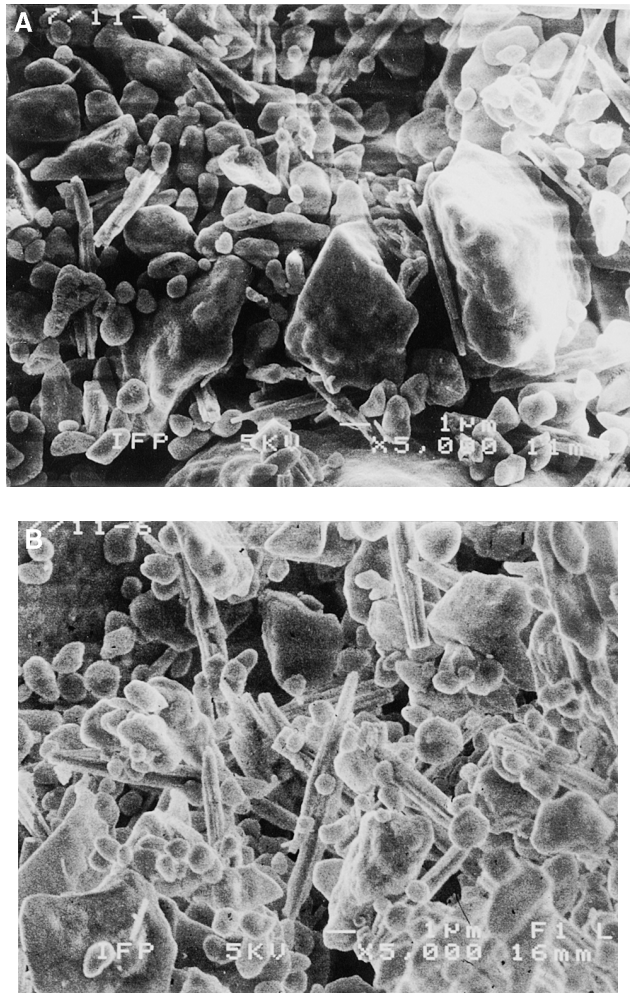

Fig. 1. SEM images. Comparison of identical samples, prepared by freezing and lyophilisation (A) or by dehydration with acetone (B).

2.3. 60

For the slurry hydrated at rest, the sample at 2 h (Fig. 5) contains rod-like crystals, whose length is of the order of 1 μm. However, they are generally smaller and thinner than the crystals observed in the corresponding sample of the agitated paste (ag60-3 or ag60-5, Figs. 6 and 7).

The following sample, taken at 5 h 30 min of hydration, is presented in Fig. 8. This sample (Fig. 5) looks quite like the previous one. Crystal creation does not seem to have progressed. Crystals remain very thin and the structure of the sample is very porous. This provides evidence for the presence of a large quantity of free water in the sample.

2.4. ag20

The first sample of this series (Fig. 9) does not contain any visible hydration products. Polymers are evident in the interparticle space and on the particle surface.

Fig. 10 presents the sample observed at 8 h 45 min of hydration. One can notice the presence of numerous spherical particles of micrometric size.

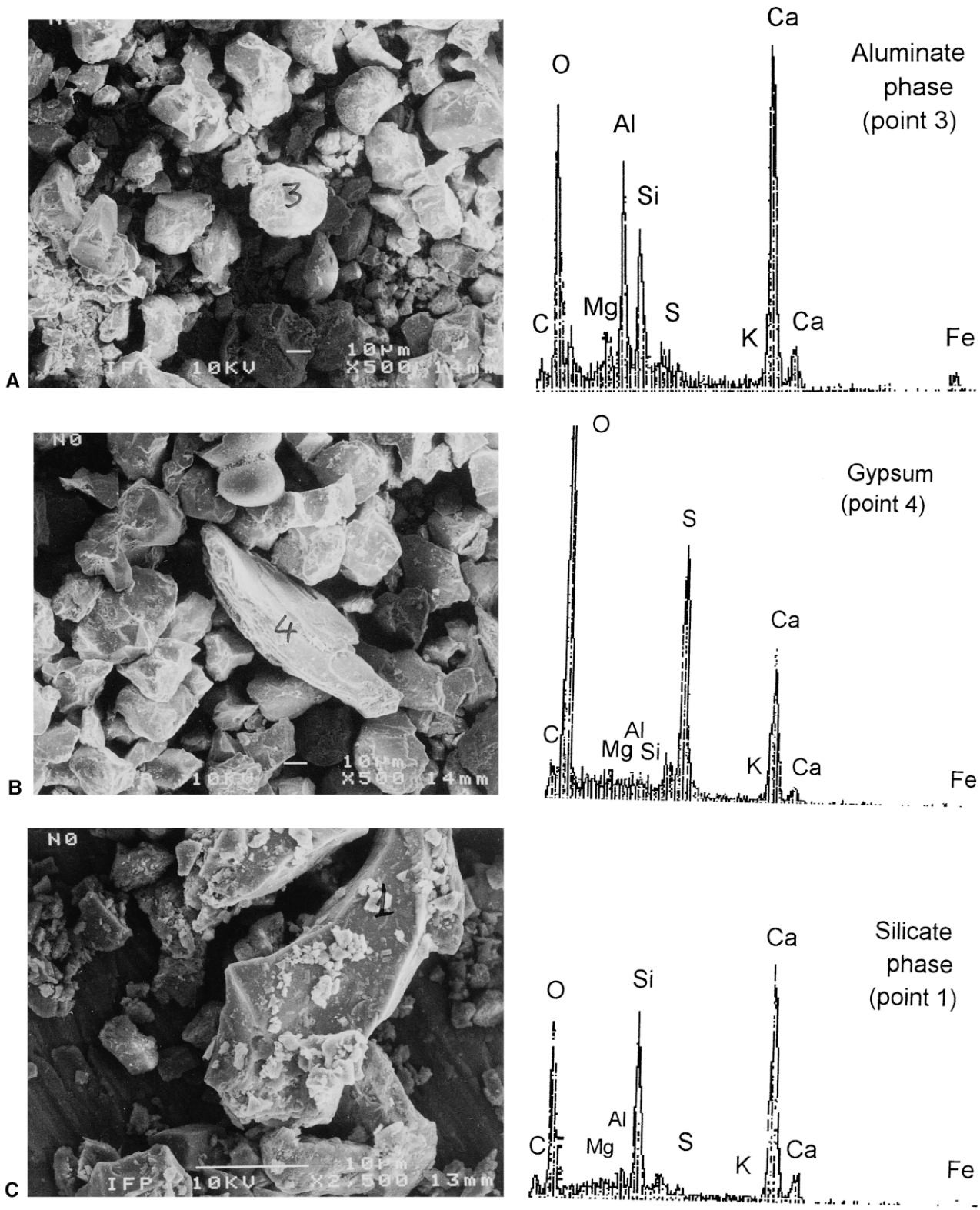

Fig. 2. (A–C) Dry cement SEM images and energy dispersive X-ray spectra.

At the end of the thickening time the sample presents a very compact aspect. Numerous spherical crystals of colloidal dimensions encumber the space between unhydrated cement grains. Their elementary analysis gives peaks of Ca, Si, Al, S, and Fe at various intensities. They probably are ettringite or monosulfate spherulites. Rod-like crystals do not appear at this temperature.

A very characteristic feature of this sample is the pres-

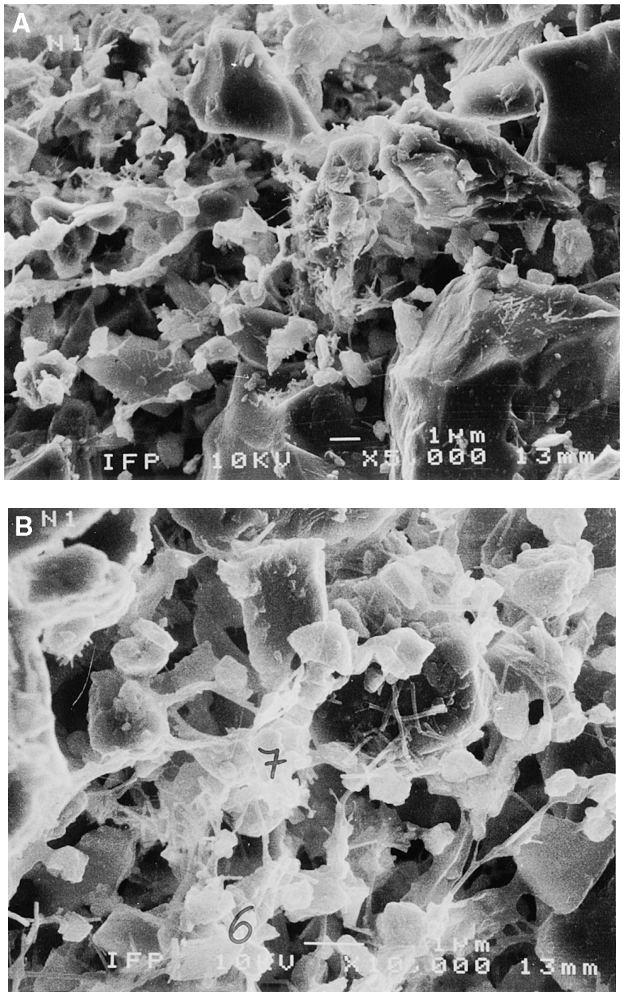

Fig. 3. (A, B) Sample ag60-1.

ence of massive calcium hydroxide crystals, which appear as thick plates that attain lengths of about 20 μm. C-S-H gel starts to cover the surface of the particles, but coating is not yet uniform.

Particles surface and even spherulites surface are entirely covered by fibrillar gel.

The sample presented in Fig. 11 was taken from the same slurry and at the same time as the one sample presented in Fig. 12, but water removal was by acetone extraction. The two methods are compared to verify that crystals and microstructure revealed are not formed as artifacts of the sample preparation method. As expected, when washing the sample with acetone, the three-dimensional arrangement of the particles and crystals crumbles down. Calcium hydroxide crystals have been smashed. However, we find again the same small spherulites and, at higher magnification, the fibrillar gel on the surface of the particles.

2.5. 20

Micrographs of the stagnant paste were observed in the microscope at 8 h 45 min and 20 h of hydration and are shown in Figs. 13 and 14.

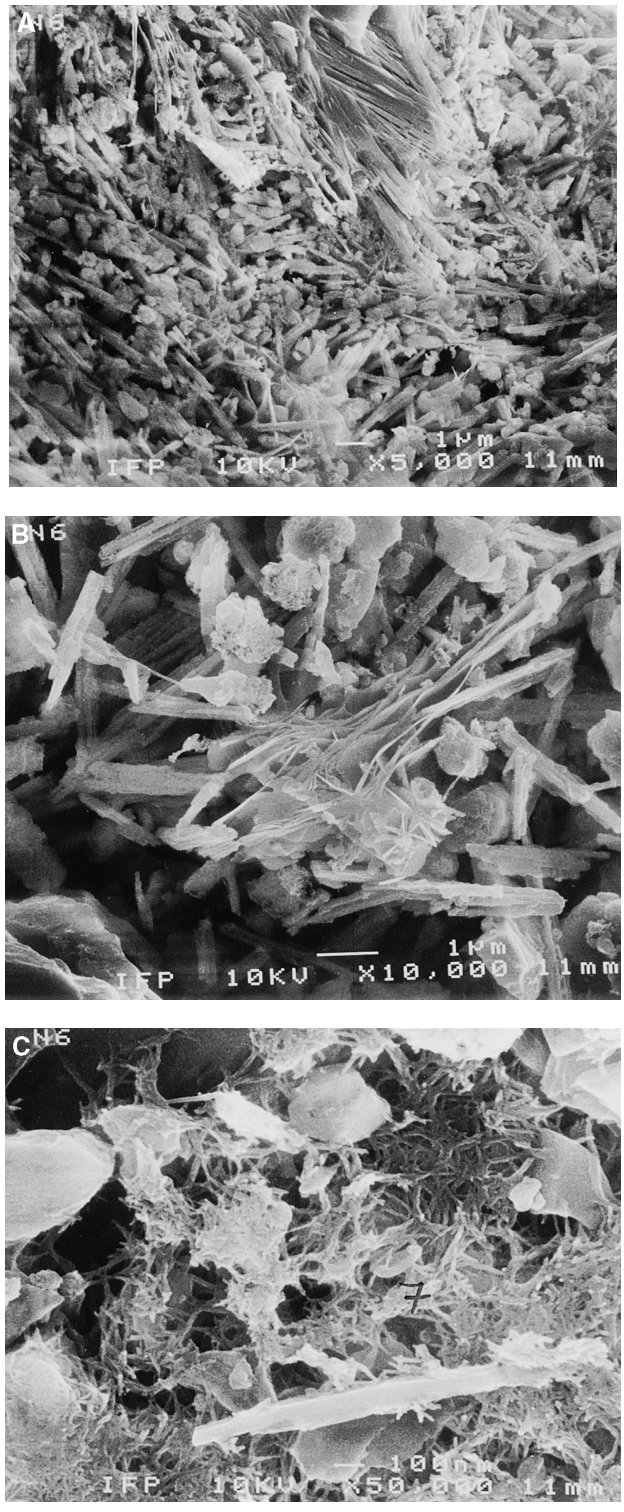

Fig. 4. (A–C) Sample ag60-6.

As for the pastes hydrated at 60°C, hydration reactions seem to be slowed considerably in the stagnant paste. Some hydration products appear at the early stages (Fig. 13), namely, a small quantity of spherulites in the interparticle spaces and tiny rod-like crystals on the grain surfaces.

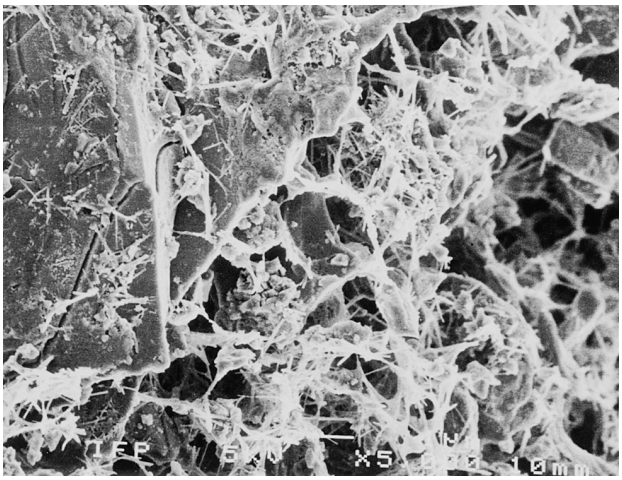

Fig. 5. Sample 60-4.

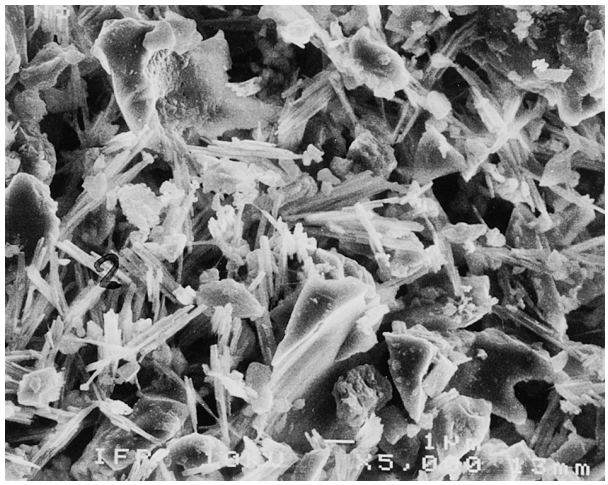

Fig. 7. Sample ag60-5 (magnification 5000×).

Twenty hours after mixing with water, the stagnant paste (Fig. 14) contains a very small quantity of hydration products compared with the sample just after mixing (Fig. 9). Polymers have almost disappeared, but no continuous structure is present, as for the corresponding agitated sample. In contrast, the large cavities observed between the cement grains can be related to the presence of a large quantity of free water in the paste.

This result leads to the conclusion that stirring promotes the hydration reaction, and that not only does it not destroy the crystals—at least ettringite crystals—but it favors their formation.

3. X-Ray diffraction analysis results

Qualitative XRD analysis was performed on some of the pastes prepared for SEM tests. The Philips PW 1820 apparatus at the IFP equipment was used. This apparatus is equipped with an incident-beam monochromator from graphite crystal and a cobalt anticathode. Data were collected over the angular range of 2ϑ of 2 to 72 degress for all samples, in steps of 0.05 degree at a fixed time of 30 s per step.

We follow, as indicators of the reaction progression, the development of the peaks corresponding to ettringite, portlandite, and gypsum, as well as the level of the bottom of the diagram, which indicates the degree of amorphization of the silicate phases.

The evolution of the diffractograms with hydration time is shown in Fig. 15, where the samples ag60-1 and ag60-6 are compared. At the end of the thickening time, ettringite and portlandite peaks present important intensities and gypsum peaks have disappeared. The presence of amorphous material (as, for example, the C-S-H gel) in the ag60-6 sample is indicated by the elevation of the bottom of the diagram.

Two samples of identical composition cured at 20°C and 60°C until the end of their thickening time (ag60-6 and ag20-6) were analyzed to evaluate the influence of temperature on the hydration process. The comparison of the dif-

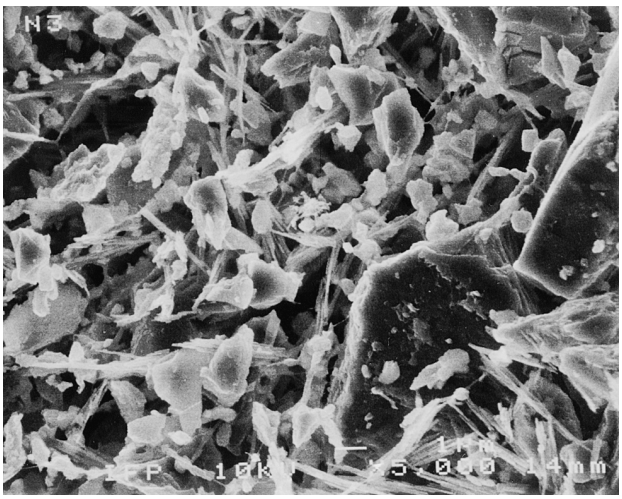

Fig. 6. Sample ag60-3 (magnification 5000×).

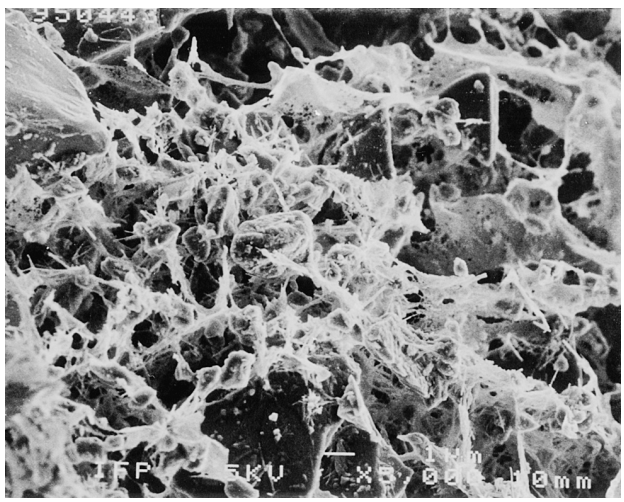

Fig. 8. Sample 60-6.

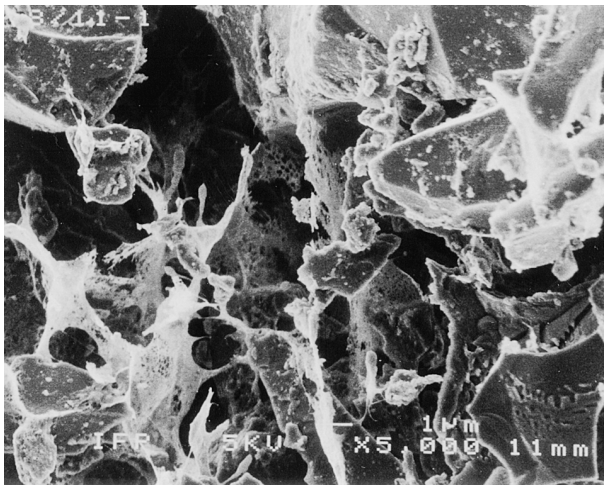

Fig. 9. Sample ag20-1 (magnification 5000×).

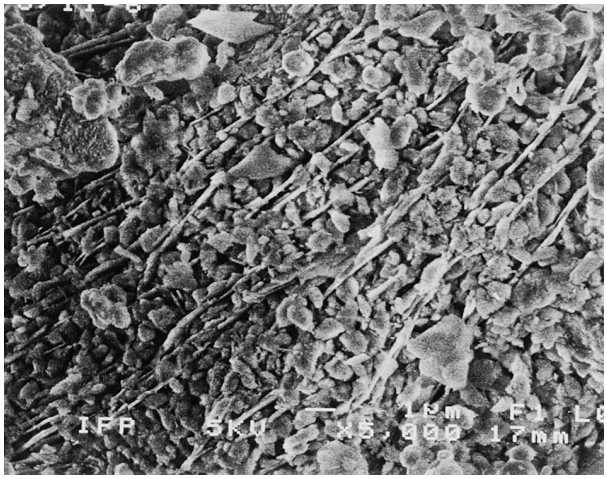

Fig. 11. Sample ag20-6, prepared by solvant extraction (magnification 5000×).

fractograms (Fig. 16) indicates that the hydration state is approximately identical in the two samples. Characteristic peaks of ettringite, portlandite, gypsum, and C_3S present almost the same intensities. These results account for the suggestion that thickening of the paste happens at the same rate of hydration for all the pastes of the same composition. However, this stage of the hydration process is achieved much more rapidly when the paste is cured at elevated temperature. For the samples analyzed, the thickening time is 6 h at 20° and 2 h 45 min at 60°C. Thus, increase of temperature accelerates considerably the hydration reaction.

As already observed by the SEM tests, the hydration process seems to be very different according to whether the slurry is at rest or stirred. This parameter is studied by comparing pastes of identical composition hydrated at rest or under agitation at 150 rpm until their thickening time. Fig. 17 compares specimens ag20-6 and 20-6. The XRD diagrams presented in these figure make clear that the rate of hydration is much more advanced for the stirred samples.

For sample ag20-6, portlandite and ettringite are detected in large amounts. A small quantity of amorphous product is also present in the sample. Gypsum is completely consumed. Sample 20-6 does not contain any detectable port-

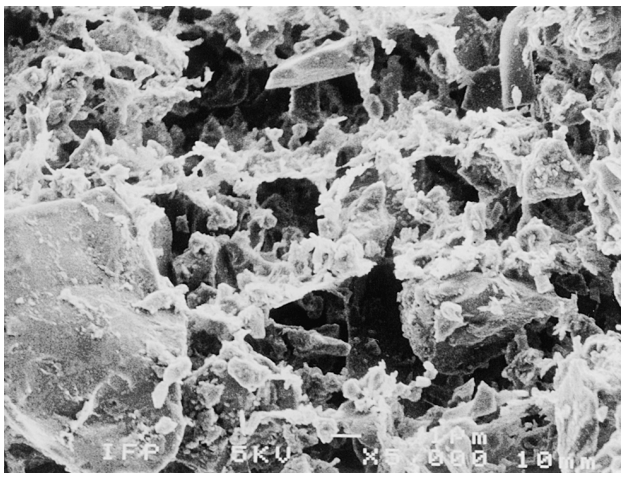

Fig. 10. Sample ag20-4 (magnification 5000×).

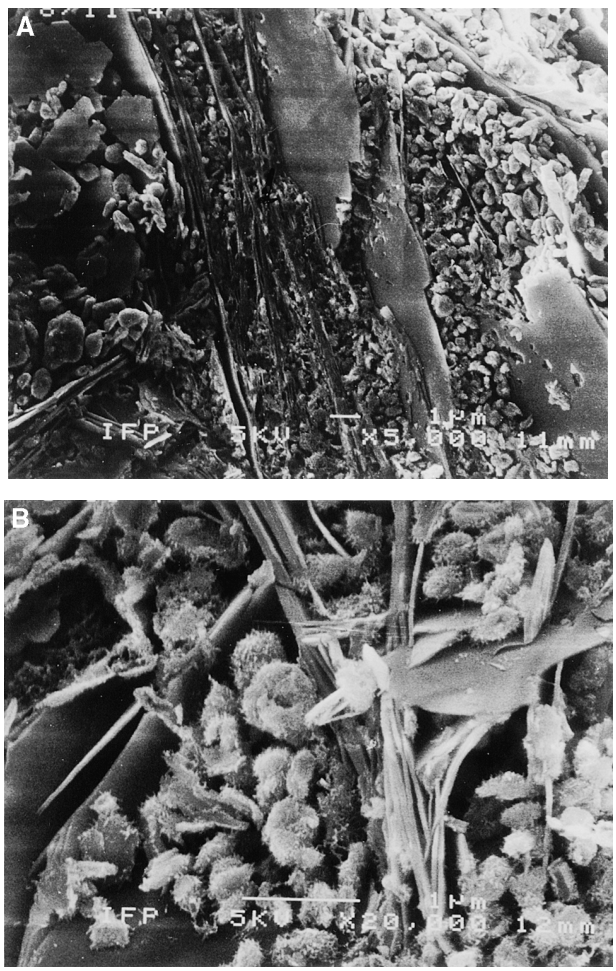

Fig. 12. (A, B) Sample ag20-6.

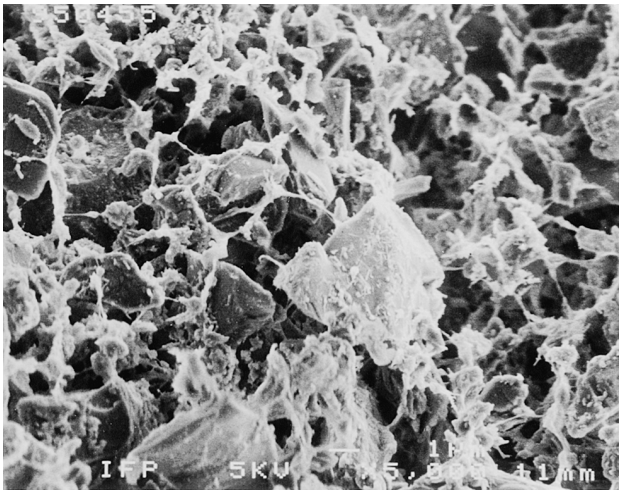

Fig. 13. Sample 20-4 (magnification 5000×).

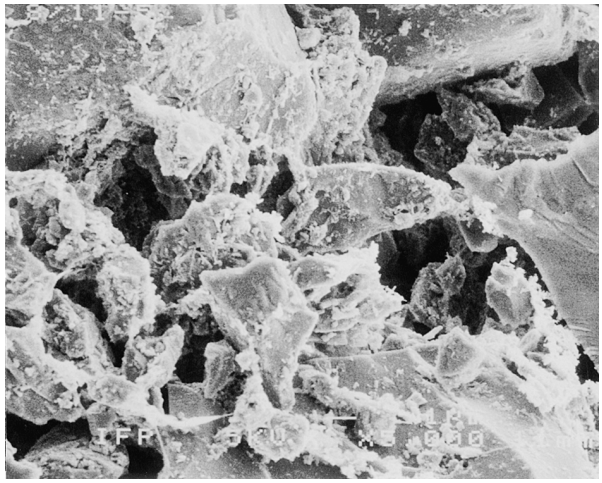

Fig. 14. Sample 20-6 (magnification 5000×).

landite. There is a small quantity of ettringite, badly organized or in the form of small crystallites, which is at the origin of broad peaks.

4. Conclusion

This is a study of the microstructural and chemical evolution of an oil well cement paste. Microstructures of the pastes were examined by optical and scanning electron microscopy. Energy dispersion X-ray spectrometry was used as an aid to identify the chemical composition of some crystals and matrices. XRD analysis was conducted to estimate the presence and relative quantity of different minerals in the paste.

The morphology of the reaction products was studied by SEM. For most of the experiments, free water was eliminated by frozen samples via lyophilization. Next, platinum-coated fractured surfaces of the samples were examined. Samples prepared by solvent extraction also were examined. The comparison of the results verified the liability of our experimental methods and the absence of method-related artifacts.

The combination of SEM observations and XRD results gives rise to the following conclusions:

- The nature and structure of the hydration products are very sensitive to the exact experimental conditions (e.g., temperature, stirring conditions, etc.). This might have an important impact on their macroscopic properties, as, for example, on their rheometric behavior [23] or their mechanical characteristics after setting.
- Stirring has a marked influence on the formed products: a large quantity of calcium sulfoaluminate particles (ettringite or monosulfoaluminate) is formed in the intergranular porosity when cement is kept stirred during the early hydration period (i.e., before setting). At 20°C these particles have mainly spherical morphology and often are trapped within large portlandite crystals. At 60°C they mainly have a rod-like morphology.

When the paste is kept stagnant, no intergranular com-

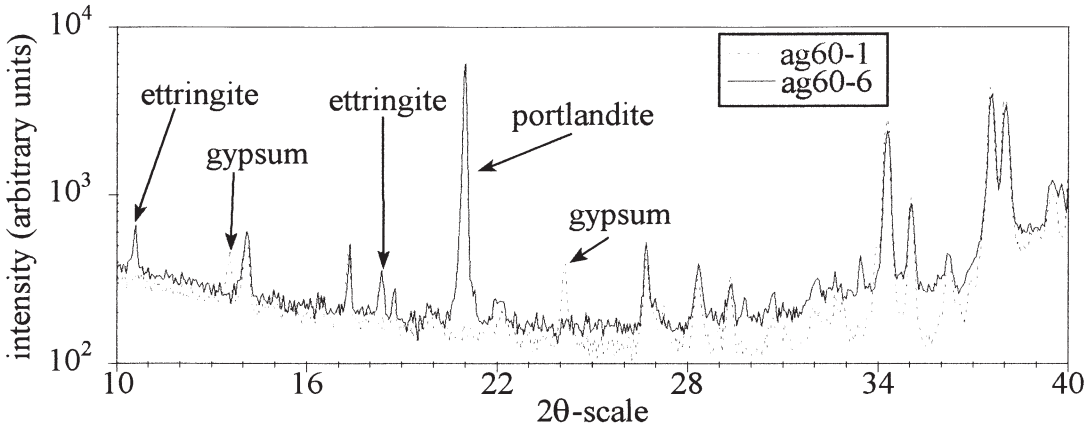

Fig. 15. Comparison of X-ray diffraction traces of a paste just after mixing or at the end of the thickening time.

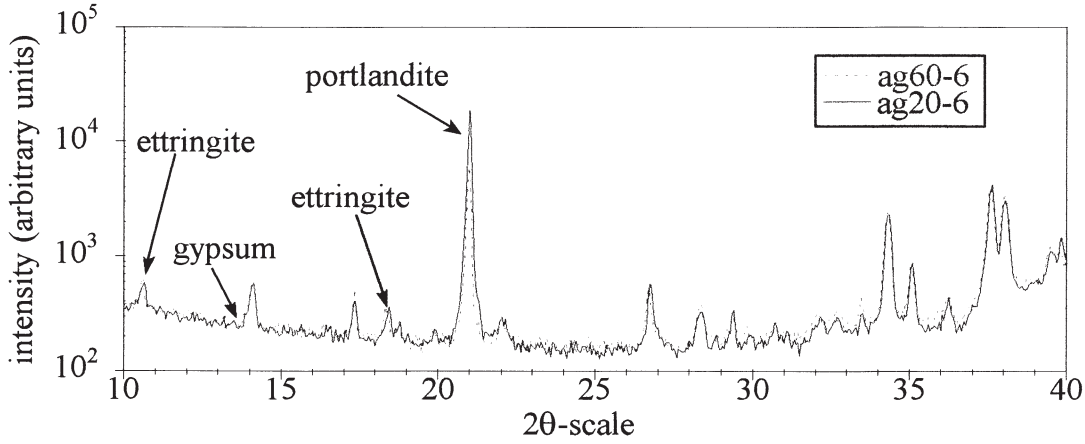

Fig. 16. Comparison of X-ray diffractions traces of a paste hydrated at 20°C or 60°C.

pounds are formed. The reaction takes place at the surface of the cement grains, leading to the formation of very fine compounds under the form of small precipitates or gel network partially covering the surface.

Dissolution of the anhydrous compounds to their ionic constituents is taking place from the surfaces of the grains. In a stagnant paste, diffusion is the main transport mechanism of the ions from the grains surface to the bulk solution, and it is not sufficiently effective in homogenizing the solution. Thus, the solution becomes supersaturated next to the grains, although still diluted in the pores. Hydrates form near the grains and, due to their low solubility, precipitate on their surface, forming a protective layer (or gel), which hinders further dissolution of the anhydrous compounds and slows down the hydration process. Because they have formed from a highly supersaturated solution, these particles are extremely small and usually have a highly disordered or even amorphous structure. In contrast, in a stirred paste, convection leads to homogeneous distribution of the ions in the solution. Consequently, hydration product crystals form both around the cement grains and away of them, following a through-solution reaction mechanism.

- Pastes studied in this work were cured either at 20°C or 60°C. This temperature range is limited. Nevertheless, it shows the high degree of dependence of the forms of the hydration products on the curing temperature. Calcium sulfoaluminate particles, which dominate in the early hydration period, are mainly spherical at 20°C and rod-like at 60°C. CH crystals are more massive at 20°C than at 60°C.

Temperature accelerates considerably the hydration process. However, as revealed by the similarity of the X-ray spectra, pastes of identical composition hydrated at 20° and 60°C present the same rate of hydration at the beginning of the setting.

Acknowledgments

We would like to acknowledge Elisabeth Rosenberg and Bernadette Rebours from the IFP, for their role in the elaboration of the experimental methods and their advise on SEM and XRD, as well as Marie-Claude Lynch for carrying out the SEM experiments. We also acknowledge the CNRS, the

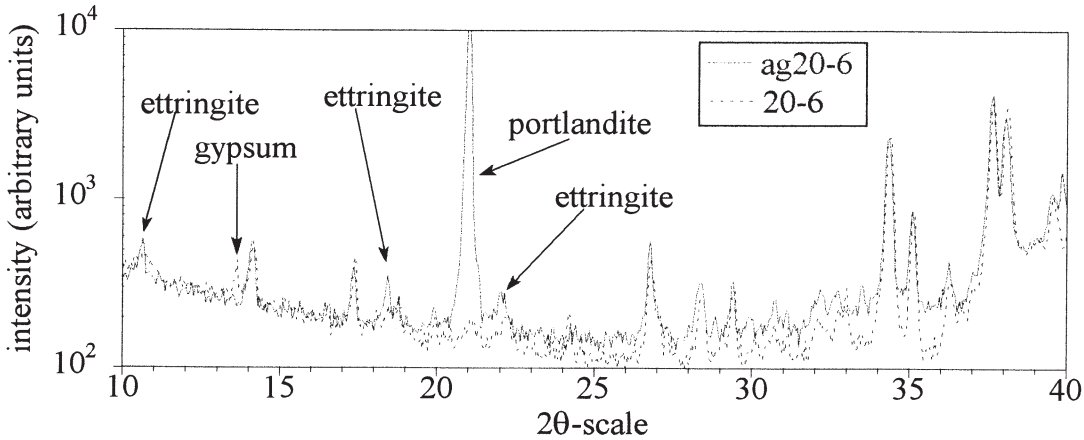

Fig. 17. Comparison of X-ray diffraction traces hydrated under stirring or at rest.

ARTEP, the UJF, the Région Rhône-Alpes and the CEE for their financial support.

References

[1] D.N. Winslow, J.M. Bukowski, J.F. Young, Cem Concr Res 24 (6) (1993) 1025–1033.
[2] K.L. Scrivener, University of London, 1984.
[3] G. De Schutter, L. Taerwe, Cem Concr Res 2 (3) (1995) 593–604.
[4] J.E. Ash, M.G. Hall, J.I. Langford, M. Mellas, Cem Concr Res 23 (2) (1993) 399–406.
[5] F. Yan, G. Ping, X. Ping, J.J. Beaudoin, Cem Concr Res 25 (1) (1995) 63–70.
[6] S.M. Clark, P. Barnes, Cem Concr Res 25 (3) (1995) 639–646.
[7] W.A. Gutteridge, Chemistry and Chemically-Related Properties of Cement, Proc Brit Ceram Soc, London, April 12–13, 1984.
[8] H.F.W. Taylor, Cement Chemistry, Academic Press, London, UK, 1991.
[9] S. Mehta, R. Jones, B. Canevy, Oil Gas J Oct. 3 (1994) 47–53.
[10] G. Ping, F. Yan, X. Ping, J.J. Beaudoin, Cem Concr Res 24 (4) (1994) 682–694.
[11] G.W. Groves, Mater Res Soc Symp Proc 85 (1987) 3–12.
[12] S.A. Rodger, G.W. Groves, N.J. Glayden, C.M. Dobson, Mater Res Soc Symp Proc 85 (1987) 12–20.
[13] P.K. Mehta, Cem Concr Res 6 (2) (1976) 169–182.
[14] E. Grusczscinski, P.W. Brown, J.V. Bothe, Cem Concr Res 23 (4) (1993) 981–987.
[15] G.H. Tattersall, P.F.G. Banfill, The Rheology of Fresh Concrete, Pitman Adv Publ Prog, London, UK, 1983.
[16] H. Uchikawa, S. Uchida, S. Hanehara, il Cemento 1 (1987) 3–22.
[17] P.V. Vlachou, Thèse de doctorat, INPG, France, 1996.
[18] J. Keating, D.J. Hannant, A.P. Hibbert, Cem Concr Res 19 (4) (1989) 554–566.
[19] S.P. Jiang, J.C. Mutin, A. Nonat, Cem Concr Res 25 (4) (1995) 779–789.
[20] F.D. Tamas, Cem Concr Res 12 (1) (1982) 115–120.
[21] American Petroleum Institute, Specification for Materials and Testing of Well Cements, API spec. 10, 3rd edition, August 1987.
[22] S. Masse, Thèse de doctorat, Univ. Pièrre et Marie Curie, 1993.
[23] P.V. Vlachou, J.M. Piau, Cem Concr Res 2 (6) (1997) 869–881.